ANALYSIS AND CLASSIFICATION OF HIGH ARCTIC GLACIERS WITH ASAR DATA

A. P. Doulgeris[1], *K. Langley*[1,2], *T. Eltoft*[1]

[1]University of Tromsø
Department of Physics and Technology
Tromsø, Norway

[2]Norwegian Polar Institute
Tromsø, Norway

ABSTRACT

We apply a polarimetric classification scheme to Envisat Alternating Polarisation mode ASAR images and compare to ground truth data. By analysing images with a range of acquisition conditions and comparing the classification accuracy with the ground truth data, we investigate the influence of the acquisition conditions for glacier facies discrimination. We find that the main influence is the image swath angle, which affects the image pixel geometry. There was no obvious preference for the different polarisation channels, although the dual polarisation classifications were consistently better than single polarisation classifications.

Index Terms— Arctic Glaciers, Classification, Ground Penetrating Radar, Polarimetric Synthetic Aperture Radar.

1. INTRODUCTION

The present state of Arctic ice masses and changes over time are of scientific and social importance because they are recognised as key indicators of climate change [1]. Identifying and monitoring fluctuations in glacier facies [2] provides a means to track climate change. The only feasible method to obtain good spatial and temporal coverage of the Arctic glaciers is through the use of satellites. Space-borne Synthetic Aperture Radar (SAR) instruments, operating independently of weather and daylight, are a particularly valuable tool in Arctic areas. At microwave frequencies the signal penetrates some distance into the glacier such that the return signal is influenced not only by the surface, but also by the shallow subsurface. In dry conditions, the backscatter signal is therefore less influenced by short term events (e.g snowfall) and more closely linked to longer term glacier facies.

The majority of glacier classification work on small glaciers and ice caps has been done with single or dual polarised SAR data. It has been shown that SAR glacier zones are related to identified glacier facies [2, 3]. Fully polarimetric data has been utilised in a number of studies although focus was not on the glaciers, rather on Alpine regions that contained glaciers [4]. The rather complex structural and textural signature of the different glacier facies makes them a prime target for more advanced polarimetric studies [5].

Our study focuses on a high Arctic glacier. We show a multivariate classification of dual polarised ASAR data that delimits the glacier facies. Images with different acquisition conditions are classified and compared to ground truth data. We describe the SAR data sets, the ground truth data and the classification schemes in Sec. 2. The classification images and accuracy results are presented and discussed in Sec. 3, and we summarise our conclusions in Sec. 4.

2. DATA AND METHODS

Our data sets consist of dual polarisation C-band Envisat ASAR data over Kongsvegen glacier, Svalbard, in both HH/HV and VV/VH polarisations, from both ascending and descending passes, and over a large range of look angles from 14 to 43 degrees (ASAR image swath angles IS1, IS3 and IS6). The raw single-look complex (SLC) data is geo-coded and multi-looked simultaneously to produce 30m resolution, 32-look covariance matrix data (MLC) images. A mask is applied to isolate the glacier pixels for classification. The twelve basic conditions studied are the combinations of: IS1, IS3 and IS6 satellite look angle; ascending (A) or descending (D) pass direction; and HHHV or VVVH dual polarisation mode. A further reduction of the dual polarisations into individual HH, HV, VH and VV channels, giving 24 combinations, is also investigated. Each combination is classified and compared to the ground truth data.

The ground truth data is derived from a network of ground penetrating radar (GPR) profiles collected in the same spring season as the ASAR images. The along glacier profiles have manually classified into 4 zones of interest [6]. The four zones are glacial ice, ”herring bone” ice, superimposed ice, and firn (Fig. 1). The ”herringbone” ice region appears as a distinctly different region on the GPR data profiles. The ground truth test score is the classification accuracy under the ground truth locations, as a percentage.

A supervised classification of each MLC image is obtained by estimating K-Wishart [7] model parameters for each class of the ground truth data. The K-Wishart is a non-Gaussian based generalisation of the Wishart distribution for covariance matrix data, assuming the raw SLC SAR data is multivariate K-distributed [8]. The raw data is modelled as

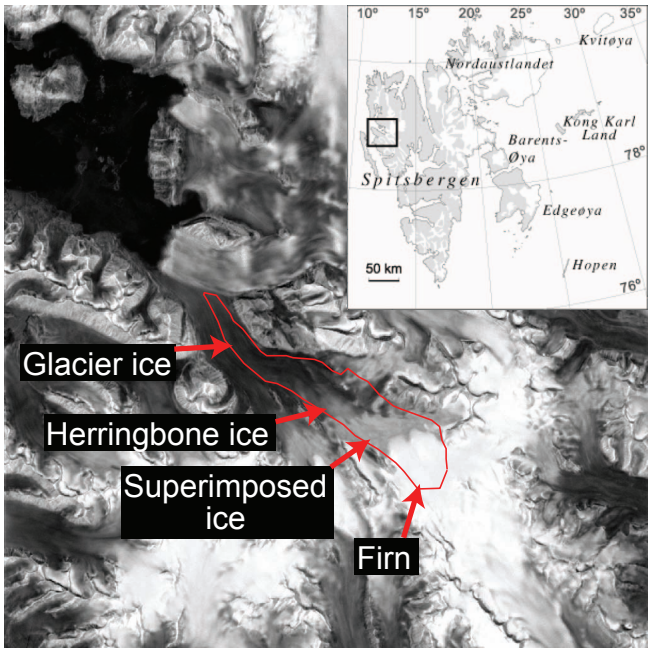

Fig. 1. Location of Kongsvegen glacier, Svalbard, and combined SAR intensity image clearly showing the four zones of interest. The glacier mask outline is shown in red.

the product of a non-Gaussian Γ-distributed 'texture' term with a multivariate Gaussian 'speckle' term [9]. This leads to the non-Gaussian based 'K-Wishart' distribution for the covariance matrix [7]. Moment based methods are used to estimate the model parameters from the covariance matrix data. The parameters can be interpreted as a mean intensity μ_z, a non-Gaussian shape term α and a normalised polarimetric term $\mathbf{\Gamma}$. The entire image is classified with a Bayesian maximum likelihood scheme using the estimated model parameters for each class. A simple median filter (3×3) is subsequently applied to smooth the classified image.

Unsupervised clustering of the sample covariance matrix data using the K-Wishart classifier is also performed. We used 7 classes for the clustering, because fewer classes had poor histogram fitting which is indicative of mixtures (see Sec. 3). The clustering result was also smoothed by median filtering. The ground truth test had to be modified to allow multiple classes to be combined into each zone for the comparison. The optimum merging method is to assign each cluster to the zone with the maximum count in the class confusion matrix, because maximising the chosen counts will minimise the total error.

The ground truth test scores are calculated and plotted, for each combination, to visualise any influence of these conditions to the classification accuracy.

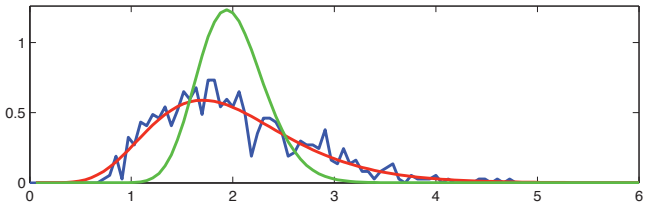

Fig. 2. Supervised class intensity histogram (blue) and a fitted Gaussian based model (green) and K-distribution based model (red).

3. RESULTS AND DISCUSSION

3.1. Supervised classification

The ground truth data consists of just over two thousand points, which is rather few for 4 class estimation. As a result, the histograms are only coarsely defined, and yet they clearly show some shape deviation from a Gaussian based (i.e. chi-squared) intensity profile (Fig. 2). Both models depict 32-look averaged MLC data, with an effective number of looks of 22.7 being the average estimated from the actual data sets. This high number of looks should make all but very extreme textures appear nearly Gaussian. We propose that the observed extreme shape is most likely due to a mixture effect, where the 4 human derived classes of interest may actually contain distinct sub-classes. Although we suggest that the 'shape' is most likely due to mixtures and not texture, the flexible K-model appears to capture the data structure very well. It turns out that both models perform similarly, which is probably due to good class separability in the intensity space.

The results for the K-Wishart supervised classification are shown in Fig. 3. The test scores (upper panel) appear to indicate that the descending pass data give better classifications, and a possible improvement, and less variability, with increasing incidence angle (IS1 to IS6). There is no clear preference for HHHV or VVVH polarisation in these few samples. The visual detail in the classification image follows the firn/superimposed ice boundary and the superimposed/herring bone ice boundary very well, however there is quite a lot of confusion in the herringbone/glacier ice boundary. Whether IS3 performs better than IS6, may also be influenced by the fact that the IS3 acquisitions have a slightly finer ground pixel resolution, 7.8 m range by 3.1 m azimuth versus 7.8 m by 3.9 m.

We interpret the main variability in the scores to be influenced by the actual ground image geometry (see Fig. 4). That is, the very poor results for IS1 ascending come from an image that is extremely stretched along the glaciers length with relatively few pixels in the cross direction and potentially less class distinguishing ability. The IS1 descending pass is stretched in the nearly cross glacier direction, resulting in many cross glacier pixels. The difference in geometry

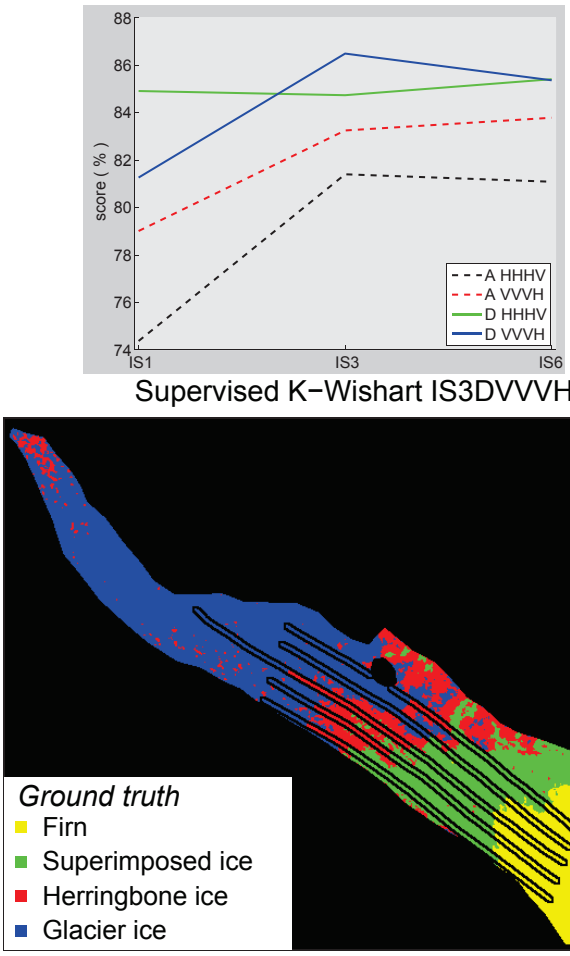

Fig. 3. Supervised, 4 class K-Wishart: scores and best classification image with the ground truth data lines overlaid.

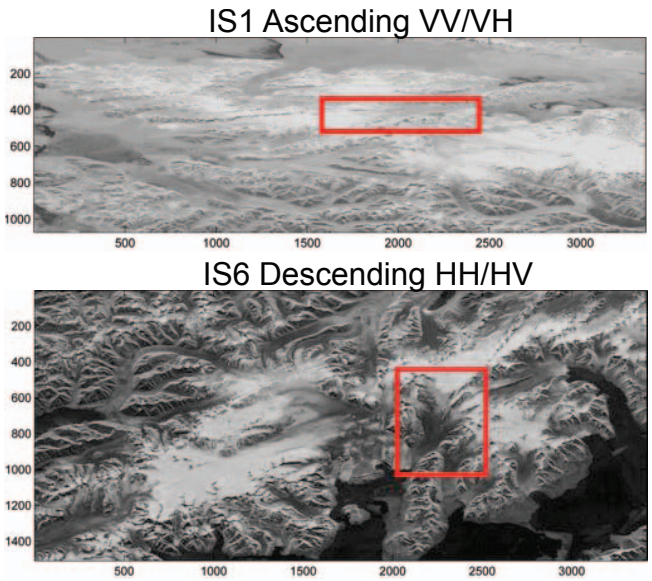

Fig. 4. Geometrical differences of acquisition conditions. The box shows the approximate extent of Kongsvegen glacier.

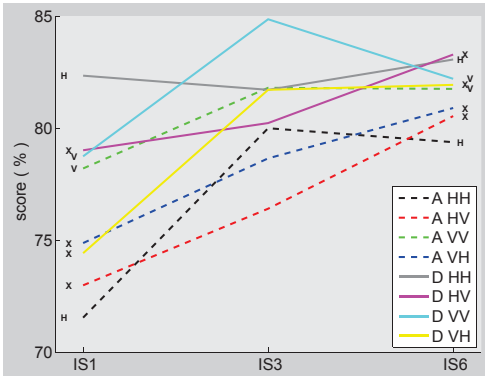

Fig. 5. Individual polarisation channel scores for supervised K-Wishart classification.

is less significant with increased incidence look angle, with very little difference between ascending or descending for the IS6 images.

The individual polarisation channel results more clearly show the improvement trend from IS1 to IS6. See Fig. 5. The descending scores are generally superior to the ascending scores, but the individual V, H or X (VH and HV) polarisations do not show any definite preference. The individual scores are a few percent lower than the dual results, as might be expected.

In summary, the supervised results indicate that the preferred condition is that which gives the best pixel geometry. In our case the descending IS3 VVVH data set, with 86.5% classification accuracy.

3.2. Unsupervised segmentation

The initial unsupervised 4 class clustering results were only moderately accurate, in the 70% range, and the modelling did not fit the intensity histograms particularly well. We observed side lumps and generally poorly matched function curves, that are usually indicative of not having cleanly separated data classes. Investigation of the model parameter space (μ_z, α and $\mathbf{\Gamma}$) and class intensity histograms led us to choosing 7 classes for the unsupervised modelling. The resulting, combined class, test score gives similar results to the supervised case, with results from the 72-85%, and also show the same preferences (Fig. 6). Even with the extra classes, the main confusion still appears to be at the herringbone/glacier ice boundary. The unknown extra classes may also be of interested on their own and require further investigation.

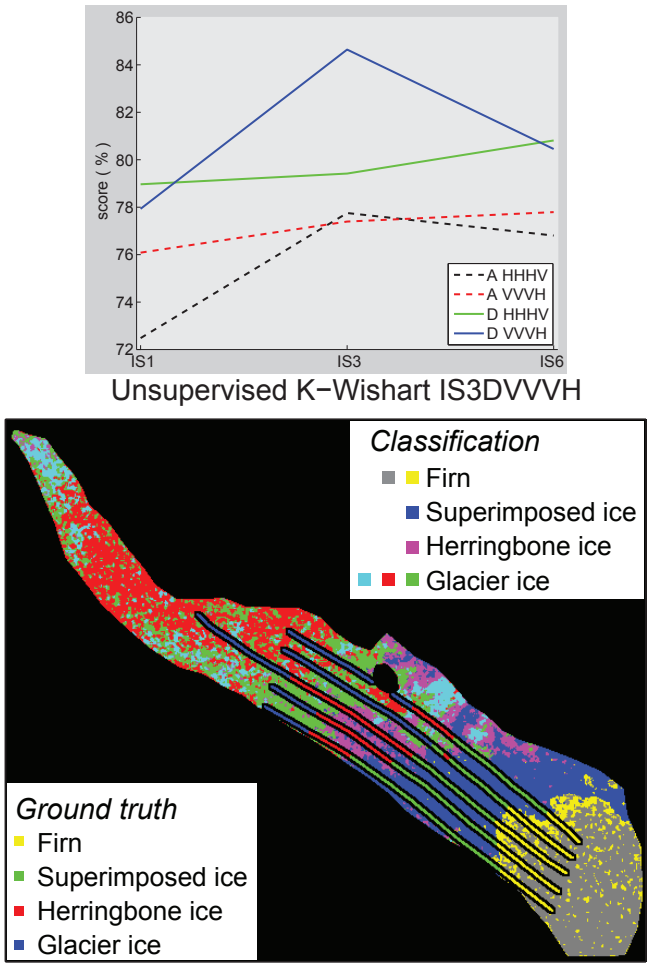

Fig. 6. Unsupervised, 7 class K-Wishart: scores and best classification image. The classification legend indicates the merging of classification classes into ground truth classes.

4. CONCLUSIONS

Results are very promising showing that the classification does discriminate the different glacier facies; firn, superiposed ice, and glacial ice. In addition the classification is sensitive enough to distinguish sub zones some of which have also been mapped by the GPR. The main confusion was found to be between the glacial ice and the herringbone ice, but this boundary is rather subjective even in the GPR profiles.

The best condition among our examples was the IS3 descending VVVH data set with 86.5% classification accuracy, and we suspect that the main influence is the image pixel geometry. There was no clear preference among the different polarisation channels, but using the dual channels was several percent better than using single channels. Presumably, there would be further increase with using fully polarimetric data.

The physical basis of the 'extra' classes requires further investigation, both numerically, with regard to the model parameter feature space, and actual ground based ice studies. The classification should also be applied to different glaciers to see whether the same parameters can be used for a general classifier, and also to investigate the distinct regions that are identified with the unsupervised method.

5. REFERENCES

[1] S. Solomon, D. Qin, M. Manning, Z. Chen, M. Marquis, K.B. Averyt, M. Tignor, and H.L. Miller, *IPCC, 2007: Climate Change 2007: The Physical Science Basis. Contribution of Working Group I to the Fourth Assessment Report of the Intergovernmental Panel on Climate Change*, Cambridge University Press, Cambridge, United Kingdom and New York, NY, USA., 2007.

[2] K. C. Partington, "Discrimination of glacier facies using multi-temporal sar data," *Journal of Glaciology*, vol. 44, pp. 42–53, 1998.

[3] M. König, J. Wadham, J. G. Winther, J. Kohler, and A. M. Nuttall, "Detection of superimposed ice on the glaciers kongsvegen and midre lovenbreen, svalbard, using sar satellite imagery," *Annals of Glaciology*, vol. 34, pp. 335–342, 2002.

[4] D. Floricioiu and H. Rott, "Seasonal and short-term variability of multifrequency, polarimetric radar backscatter of alpine terrain from sir-c/x-sar and airsar data," *IEEE Trans. Geosci. Remote Sens.*, vol. 39, pp. 2634–2648, Dec 2001.

[5] O. Stebler, A. Schwerzmann, M. Luthi, E. Meier, and D. Nuesch, "Pol-insar observations from an alpine glacier in the cold infiltration zone at l- and p-band," *Ieee Geoscience and Remote Sensing Letters*, vol. 2, pp. 357–361, Jul 2005.

[6] K. Langley, S.-E. Hamran, K. A. Høgda, R. Storvold, O. Brandt, J. Kohler, and J. O. Hagen, "From glacier facies to sar backscatter zones via gpr," *IEEE Trans. Geosci. Remote Sens.*, vol. Accepted, 2008.

[7] Anthony. P. Doulgeris, Stian Normann Anfinsen, and Torbjørn Eltoft, "Classification with a non-Gaussian model for PolSAR data," To be published in *IEEE Trans. Geosci. Remote Sens.*, vol. 46, no. 10, 2008.

[8] S. H. Yueh, J. A. Kong, J. K. Jao, R. T. Shin, and L. M. Novak, "K-Distribution and polarimetric terrain radar clutter," *J. Electro. Waves Applic.*, vol. 3, pp. 747–768, 1989.

[9] C. Oliver and S. Quegan, *Understanding Synthetic Aperture Radar Images*, SciTech Publishing, Raleigh, USA, 2nd edition, 2004.